

“Analysis of the Effects of Alkaline Hydrolysis Cremation on Mineral and Trace Metals in Bone”

An Honors Thesis

by

Rebekah N. Quickel

California, Pennsylvania

2017

California University of Pennsylvania

California, Pennsylvania

We hereby approve the Honors Thesis of

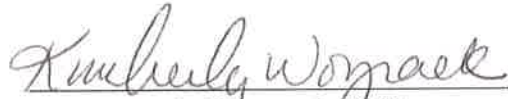
Rebekah N. Quickel

Candidate for the degree of Bachelor of Science

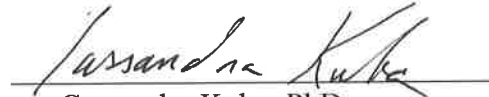
Date

Faculty


4-11-17


Kimberly Woznack, PhD
Honors Thesis Advisor


4-11-17


Cassandra Kuba, PhD
Second Reader


4-11-17


Gregg Gould, PhD
Honors Advisory Board

11 April 2017


Craig Fox, PhD
Associate Director, Honors Program

11 April 2017


M. G. Aune, PhD
Director, Honors Program

Analysis of the Effect of Alkaline Hydrolysis Cremation on

Minerals and Trace Metals in Bone

Senior Honors Thesis

Rebekah Quickel

Chemistry and Physics Department

California University of Pennsylvania

May 11, 2017

Abstract:

This research seeks to determine the changes that occur in bone during the Alkaline Hydrolysis Cremation (AHC) process. AHC is a form of cremation which is considered by many to be an environmentally friendly alternative to traditional fire cremation. AHC is typically performed in a strongly basic solution under increased pressure and temperature to accelerate the natural decomposition a body typically undergoes. This process results in human or animal remains being completely decomposed with only bone ash remaining, which can be returned to the family. The AHC process was performed using pig femur bones in a pressure cooker with a potassium hydroxide solution to mimic the commercial process. Bone structure was analyzed qualitatively by visual inspection of the bones and quantitatively by monitoring the concentrations of calcium, magnesium, and iron ions during the AHC process. Metal ion analysis was performed using atomic absorption spectroscopy. The concentration of calcium fell within the range of 30.3 ppm to 125.0 ppm, the iron concentration ranged from 17.5 ppm to 68.0 ppm, and the magnesium concentration ranged from 7.65 ppm to 24.3 ppm.

Introduction:

For as long as humans have been alive, they have also been dying. Some of the earliest cases of ritual burial of the dead can be found at sites occupied by *Homo neanderthalensis*, or Neanderthals, over 50,000 years ago.¹ This form of symbolic burial has never been seen at other sites of known prehistoric occupation and shows it to be a human specific trait. The practice of burial as a funerary process did not end with the Neanderthal extinction. Burial is the most popular form of funerary practice in the United States and as of 2005, over 61.4% of deceased individuals were buried.² Typical burials involve the deceased individual being placed in a coffin or other vessel and being placed in the ground. Often the site is marked with a headstone or marker so that others do not accidentally disturb the remains by not knowing they are present. While burial remains the most common form of funerary practice in the United States, preferences are changing. Over the years, new techniques have been developed and used as an alternative funerary process for those opposed to burial.

The second most popular funerary practice in the United States is traditional fire cremation. This technique breaks down the deceased so that the residual remains can be returned to the family. The body is broken down in a furnace where it undergoes a combustion reaction with natural gas and the body as the fuel sources. After the reaction goes to completion, the bones are still mostly solid and must be crushed into bone ash, or small, broken down particles of bone, to be returned to the family.³ Over the past years, fire cremation has steadily become a more favorable funerary practice in the United States, with a projected 58% of individuals being cremated in 2020, up from 32.3% in 2005.² The reasoning behind the switch from traditional burials to cremation can be due

to many factors, including religious and personal reasons. The lower cost for cremation over burial, a difference of over \$1,000, can also be the deciding factor for many families.⁴

More recently, a new movement for environmentally friendly funerary practices has led individuals to improve on the traditional burial and cremation practices already widely used in the United States and around the world. Traditional fire cremations release a large amount of carbon dioxide gas into the atmosphere and any plastics intentionally or inadvertently left in the casket before cremation end up being vaporized to produce toxic fumes that are also released into the environment. Medical implants, such as hip and knee replacements or pacemakers, and prosthetics must be removed from the deceased before cremation as they can contain batteries which can lead to explosive ruptures when exposed to extreme temperatures, such as those created during the cremation process.⁵ Removal of such implants can incur additional costs for the family depending on their situation.

In order to find a “greener” treatment of humans remains, the alkaline hydrolysis cremation (AHC) process was developed. This newer technique has been in use since the 1990’s by many research universities to dispose of donated corpses and deceased animals used in disease research. This form of cremation uses an alkaline hydrolysis reaction of aqueous solutions of potassium hydroxide or sodium hydroxide to break down the body into its basic, soluble, organic components and bone ash. At room temperature and pressure, this reaction can take up to twelve hours to fully decompose a human body; when the temperature and pressure are raised, the reaction rate increases to the point where a whole human body will decompose in just three hours.⁶ A typical AHC retort can

be seen in Figure 1 below. The machine has a similar style to a traditional cremation retort except for the heating coils in place of the flame ignition source and an area for the alkali solution to be introduced to the chamber. The flesh of the body is first impacted by the alkali solution, causing the cells to rupture and begin breaking down into smaller organic molecules. Once the flesh is dissolved, the solution attacks the bone.

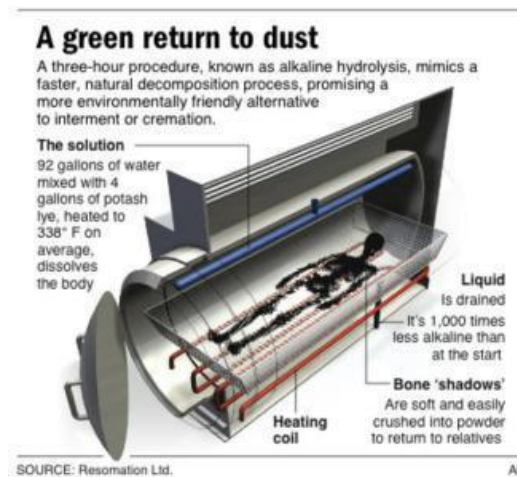


Figure 1: AHC retort/machine used to contain the remains and alkaline solution. The machine allows for a specific temperature and pressure to be achieved for efficient cremation.⁷



Figure 2: Image on the left is a form of bone ash that remains after completion of alkaline hydrolysis cremation. Although the bone is already in extremely small pieces, it can be further crushed to be returned to the family.⁸ Image on the right is crushed bone resulting from this experiment, after the AHC process and dried.

The remaining bone, which can be seen in Figure 2 above, is brittle and soft which allows the bone to be further crushed, if necessary, to be returned to the family. The end result is an organic solution with a basic pH that can be neutralized for use as fertilizer in gardens or other allowed areas. While the entire process requires heating, the carbon dioxide emissions created during the reaction are minimal when compared to fire cremation, and pose little threat to the environment. Medical implants and prosthetics do not have to be removed since they are not harmed during the reaction and can be removed from the bones afterwards, reducing costs for their removal.

This technique can also destroy infectious disease precursors, which are difficult to destroy using an incinerator. It was found that prion proteins can be inactivated using sodium hydroxide with a detergent, such as sarkosyl, and is typically used as a foaming agent in cleaning products. The detergent strips the outer layer of the prion protein, giving the base more surface area to react and breakdown the prion into amino acids and other small molecules.⁹ This makes AHC the ideal technique for disposal of infectious waste and animal carcasses used for research purposes.

Even though the immediate reaction between the body and the alkaline solution is the breakdown of the flesh and organic tissue, when the flesh is gone, the base reacts with the skeleton, which is much harder to dissolve. Bone is composed of a number of organic and inorganic components, contributing to the strength and stability of bone which causes it to be difficult to break down.

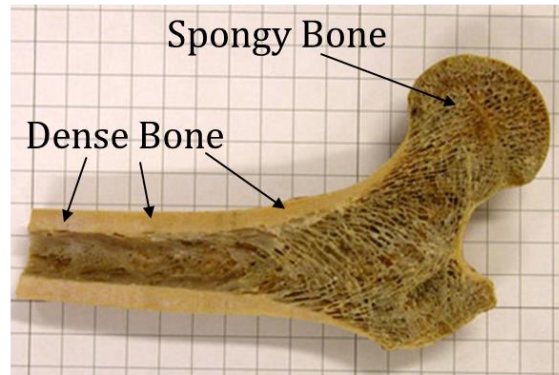


Figure 3: Cross section of the right proximal femur. The dense bone covers the outer surface of the bone and thickens as it moves downward from the femoral head. The spongy bone remains in the head and greater trochanter and extends to the marrow channel.¹¹

The densest bones in the human body are long bones; the ones found in the limbs. As seen above in Figure 3, the general composition of bone is a thick layer of cortical or dense bone that gives the outward appearance and solidity of the bone. At the proximal and distal ends are lighter portions of bone called trabecular or spongy bone. This light and airy portion of bone has a lattice work appearance and has many vacancies. These open areas allow the spongy bone to absorb impact forces in high impact areas of the body, such as the joints and balls of the feet. Without the spongy bone cushioning the ends of the bones, the dense bone would fracture under much less force.¹⁰

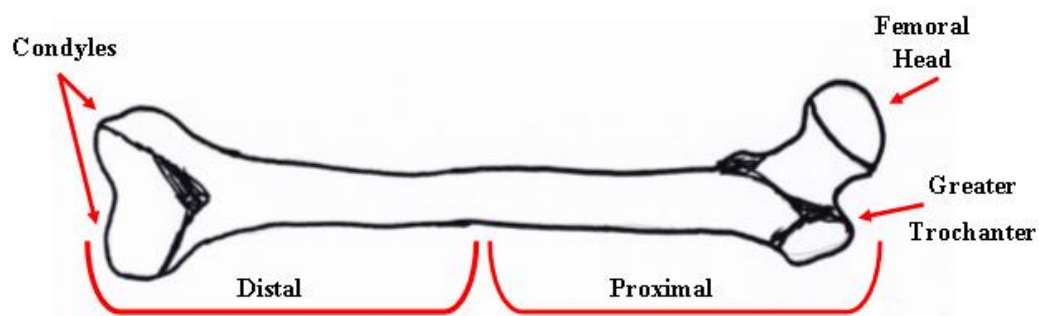


Figure 4: Summary of femoral bone landmarks, head, greater trochanter, and condyles, and direction. Proximal refers to the upper half of the femur while the distal end refers to the lower half of the bone.

The areas of spongy bone present in the long bones correspond to the locations of the epiphyses, or growth plates in long bones. In Figure 4 above, there are three areas corresponding to the growth plates, the condyles, femoral head, and greater trochanter. These three sections of the bone are not fused to the femur shaft at birth, rather they fuse later in life, between 15 to 20 years old, which makes growth plate fusion a useful indicator for age estimation. The condyles lie on the distal portion of the femur, or closer to the knee, while the head and greater trochanter lie on the proximal end, closer to the pelvis.

The microscopic organization of the dense bone includes osteons, allowing for blood vessels which feed the bone and marrow, to pass through to the bone center. Those blood vessels also feed osteocytes residing within the osteon.¹² Osteocytes control the formation and removal of bone through the signaling of osteoblast and osteoclast cells. The osteoblast cells build up bone, while osteoclasts cause bone resorption. Osteocytes are most important in bone repair after a break or fracture due to their job in signaling bone healing. The organization of these osteons and osteocytes can be seen below in Figure 5 in the cross section of a long bone. When the osteocytes stop functioning properly, due to injury or deformation, the bone strength and structure can be affected by deformation or loss of mineral components.¹⁰

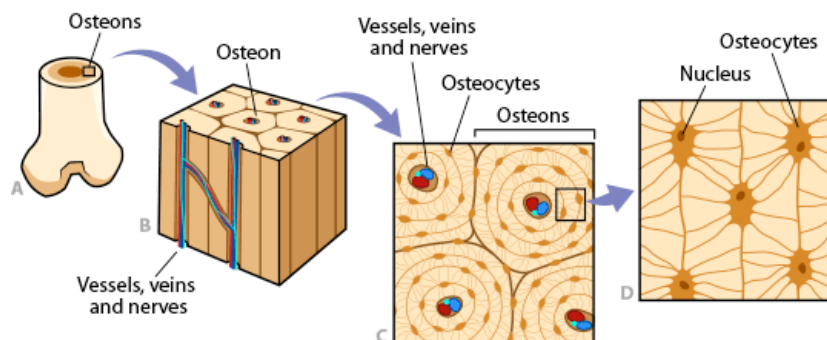


Figure 5: Breakdown of bone structure showing the collection of osteons and osteocytes.¹³

While the osteons and osteocytes give bone its structure, the strength of the bone comes from its organic and inorganic material. The largest organic component present in every human and animal bone is collagen, a large protein molecule that gives bone its flexibility.¹⁴ At birth, bone is composed entirely of collagen fibers, which intertwine to form the bone structure. As the individual and bone ages, the collagen fibers begin to be replaced with a hard, dense, inorganic mineral called hydroxyapatite.

Hydroxyapatite, $\text{Ca}_{10}(\text{PO}_4)_6(\text{OH})_2$, is a member of the apatite mineral family whose main component is calcium phosphate.¹⁵ In early bone development, pockets of hydroxyapatite are stored within the collagen fibers as they are created. As the bone ages, the hydroxyapatite mineral covers the collagen fibers and creates the dense bone structure that is most commonly seen.¹⁴ This mineral is the main component used in bone remodeling and is synthesized by the osteoblasts to heal fractures or add material for bone growth. It can also be broken down by the osteoclast cells when mineral needs to be removed from the bone surface.¹⁵

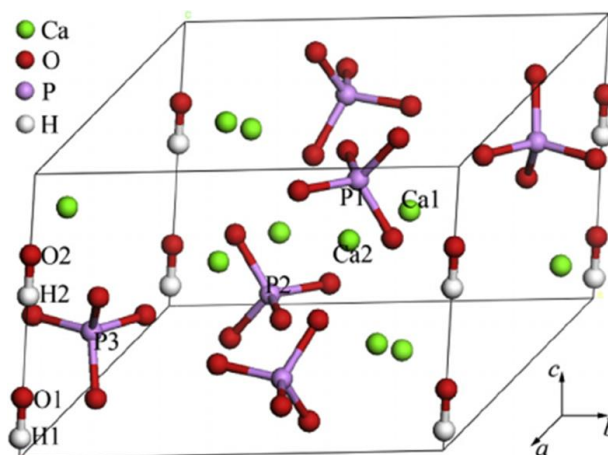


Figure 6: Crystal structure of calcium phosphate mineral with a hexagonal unit cell.^{17, 18}

The crystal structure of hydroxyapatite, seen in Figure 6, is only 50 nm in size with lattice parameters of $a=9.436 \text{ \AA}$ and $c=6.882 \text{ \AA}$. Groups of phosphates and alcohols bound to their respective hydrogens are shown.¹⁶ However, all the groups, including the calcium ions, are not bound to each other. This allows all three components of hydroxyapatite to be exchangeable for other ions or groups. The ion and group exchanges change the function of the hydroxyapatite in that particular spot and can cause it to build or destroy bone. Some of the exchanges that are possible are magnesium, zinc, strontium, and iron for calcium, carbonate groups for the phosphates, and also fluorine for the alcohol groups.¹⁵

The metal exchanges in the crystal structure have a large impact on the mineral and bone structure. Strontium has been seen to stabilize the bone structure and also stimulates bone formation and works to prevent bone loss. On the other hand, zinc has been found to help maintain healthy bone and is vital to protein synthesis within bone.¹⁵ Both of these metals contribute to changes within bone, but neither help with bone strength and stabilization. Magnesium and iron have been found to influence both of those characteristics. Iron is essential for collagen synthesis, keeping the bone slightly

flexible, so it does not break when force is applied. It can also prevent bone resorption helping to increase the strength of bone by preventing bone mass loss and boosting hydroxyapatite synthesis.¹⁵ Magnesium, on the other hand, controls osteoblast and osteoclast activity through signaling. The magnesium ions can reside on the surface of the hydroxyapatite or within the apatite structure, which increases the strength of the bone.¹⁹

The research presented here focuses on the alkaline hydrolysis reaction with bone. While the use of an acidic solution as the reactant with bone is typically considered for disposal, it removes the hydroxyapatite mineral from bone and leaves the collagen behind. This results in a flexible and bendable bone being left over, which is difficult to further break down.¹⁴ The use of a basic solution with bone employs a reaction like that shown below in Figure 7.

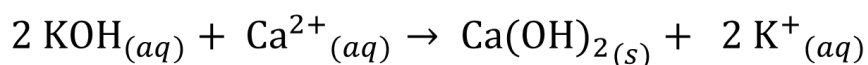


Figure 7: Alkaline hydrolysis reaction between potassium hydroxide and calcium ions from the hydroxyapatite bone structure.²⁰

In this reaction, the potassium hydroxide or sodium hydroxide, depending on the experimental conditions, will dissociate into aqueous K^{+} and OH^{-} . The OH^{-} will react and bind with the Ca^{2+} within the hydroxyapatite structure in a 2:1 ratio of hydroxide ions to calcium ions. The resulting calcium hydroxide will form a solid and precipitate out of the basic solution, effectively removing the calcium from the crystal lattice structure and leaving a vacancy in its place. The potassium ions can also bond with the PO_4^{3-} groups, in a 3:1 ratio, creating soluble K_3PO_4 . Solubilizing the phosphate could further destabilize the hydroxyapatite structure.

Theoretically, this calcium ion vacancy should result in the degradation of the bone structure and lead to the bone ash that remains after the AHC process is complete. Some research suggests that the vacancies left behind by the calcium being removed allows other cations to fill the vacancies, thus changing the bone characteristics. In the reaction above in Figure 7, the K^+ would fill those Ca^{2+} vacancies and not cause the bone to degrade. Instead, it is possible that the K^+ , or other cations, could make the bone structure stronger, based on the type of ion that takes the place of calcium.²⁰ Nevertheless, for the AHC process to successfully decompose a human or animal carcass, something must change within the bone structure that causes it to break down. It is possible that the removal of the calcium ions creates so many vacancies that only a few of the vacancies can be filled and, therefore, the unfilled vacancies still cause the bone to breakdown during the AHC process.

Another way to monitor the bone decomposition during AHC is to track the removal of ions from the bone. This can be done by detecting the concentration of the metal ions present in the resulting reaction solution. Since calcium can be removed from the bone and cause it to begin to break apart, the removal of other metals, such as magnesium and iron, that are essential to bone structure and strength, could also occur. Since magnesium can reside within the hydroxyapatite structure and on its surface, the presence of magnesium can be an indicator that the hydroxyapatite structure is beginning to decompose since magnesium is being released.¹⁹ The same can be done with iron, when iron is detected in the reaction solution the bone structure is breaking down.

A useful method for detection of metals in solution is atomic absorption spectroscopy. Atomic absorption spectroscopy converts a solution sample into an atomic

gas by burning off the rest of the solution using a flame or other thermal source. The atoms are then bombarded with monochromatic photons and the amount of light absorbed by the atomized sample is detected. By using the absorbance and a Beer's Law plot of absorbance vs. concentration, the concentration of the sample can be determined. A plethora of metals can be detected using atomic absorption spectroscopy with high accuracy.²¹

The objectives of this research were to first successfully cremate a pig femur bone, then to identify the changes that occur to the bone structure during the AHC process by monitoring the change in calcium, iron, and magnesium ions being removed from the bone throughout the AHC process.

Procedure:

This experimental procedure was adapted from the procedure by Wang and associates,²² which looked to produce the optimal conditions to perform AHC. A Presto 01370 8-Qt Stainless Steel pressure cooker was obtained and fitted with a dual temperature/pressure gauge to monitor temperature and pressure changes during the experiment. A Durabrand Single Burner 1100 watts Variable Temperature Control heating element (WS 100) was used for the heating element. The set-up can be seen in Figure 8 below.

Pig bones were used in place of human bones for this experiment since pigs are often used as a suitable model for humans in research. Four femur bones were obtained from Cheplic Meat Processing and analyzed for trauma due to the butchering process. Each bone was weighed prior to cremation and placed in the middle of the pressure

cooker. A 2 liter solution of 0.89 M potassium hydroxide (KOH) was added to the pressure cooker and filled with an additional 1.5 liters of deionized water to fill the pressure cooker halfway and prevent the cooker from running dry. The bone set up can be seen in Figure 9 below. The pressure cooker was heated for a total of three hours and depressurized every thirty minutes to remove a sample for later analysis using atomic absorption spectroscopy.



Figure 8: Pressure cookers set up with attached gauge and heating element.



Figure 9: Placement of pig femur bone, filled halfway with 3.5 L KOH/H₂O.

Bone Trauma:

Each of the four pig femurs was received with noticeable signs of trauma caused by the butchering process. Any trauma to the bone before cremation began could have impacted the length of time and extent of cremation. Any impact to the cartilage surrounding the bone should have no impact on cremation, while deeper trauma impacting the trabecular or cortical bone will introduce an additional entrance point for the KOH solution and speed up the cremation process. All femurs were sided, weighed, and measured for femur length, head diameter, and diameter at mid-shaft and can be seen in Table 1 below. All trauma was recorded for future analysis and can be seen in Table 2

and images of the trauma can be seen in Appendix A. All femurs appeared to have fused epiphyses, indicating an adult pig.

Femur Designation	Side	Weight (g)	Femur Length (cm)	Head Diameter (mm)	Diameter at Mid-Shaft (cm)
1	Right	373.81	19.6	38.0	8.9
2	Left	472.43	20.4	37.2	10.4
3	Left	488.93	20.5	41.5	10.4
4	Left	453.66	20.3	37.0	9.3

Table 1: Femur sides, weights, and measurements.

Femur Designation	Trauma
1	Slice to the posterior, medial condyle impacting trabecular bone. Superficial slice to medial surface of head, extending slightly to the neck. Slight incision of the shaft, superior to the patellar surface, lateral side.
2	Superficial slice to medial surface of the femoral head, impacting cartilage.
3	Slight shave off of condyle, more so on the medial side than lateral side, impacts trabecular bone.
4	Slight laceration on head extending to the neck. Scrape off the top head, exposing trabecular surface.

Table 2: Trauma recorded for each femur bone prior to cremation.

Atomic Absorption Spectroscopy:

All samples were analyzed using a Shimadzu AA-7000 atomic absorption spectrometer with and ASC-7000 Shimadzu auto sampler. To analyze the AHC samples by atomic absorption (AA) spectroscopy, the samples required acidification prior to dilution. A 5 mL portion of the collected sample was mixed with 5 mL of 0.8 M HNO₃ in a 10 mL volumetric flask. The samples then had to be filtered using gravity filtration due to a brown foam forming with a peroxide odor on the surface of the liquid sample. From the 10 mL sample, one mL was removed and diluted with deionized water in a 25 mL volumetric flask. The 25 mL sample were used for AA analysis.

Results:

A total of three cremations were performed and each will be discussed below.

Femur 1:

This femur was the smallest bone of the four and was used as an initial trial to test the experimental set-up and procedure before the rest of the bones were tested. Using the smallest femur also eliminated femur size and weight as a variable to influence extent of cremation. As described above in the procedure, the pressure cooker was only filled with 2 liters of 0.89 M KOH solution as outlined by Wang and associates²² and left undisturbed for three hours to determine what affect depressurizing the pressure cooker will have on the extent of cremation. After two and a half hours had elapsed, the steady stream of pressure coming from the release valve was interrupted and a yellow substance began to spew out the valve. The heat was immediately turned off and the cooker depressurized. The result of the first trial can be seen in Figure 10 below.



Figure 10: Result of yellow substance spewing from the release valve of the pressure cooker, coating the lid and fume hood sash in the substance.

After the lid was removed, the pressure cooker revealed a dark red solution along with the bone. Even though the cremation did not proceed for the full three hours, the resulting bone still showed signs of breakdown and can be seen in Figure 11 below.

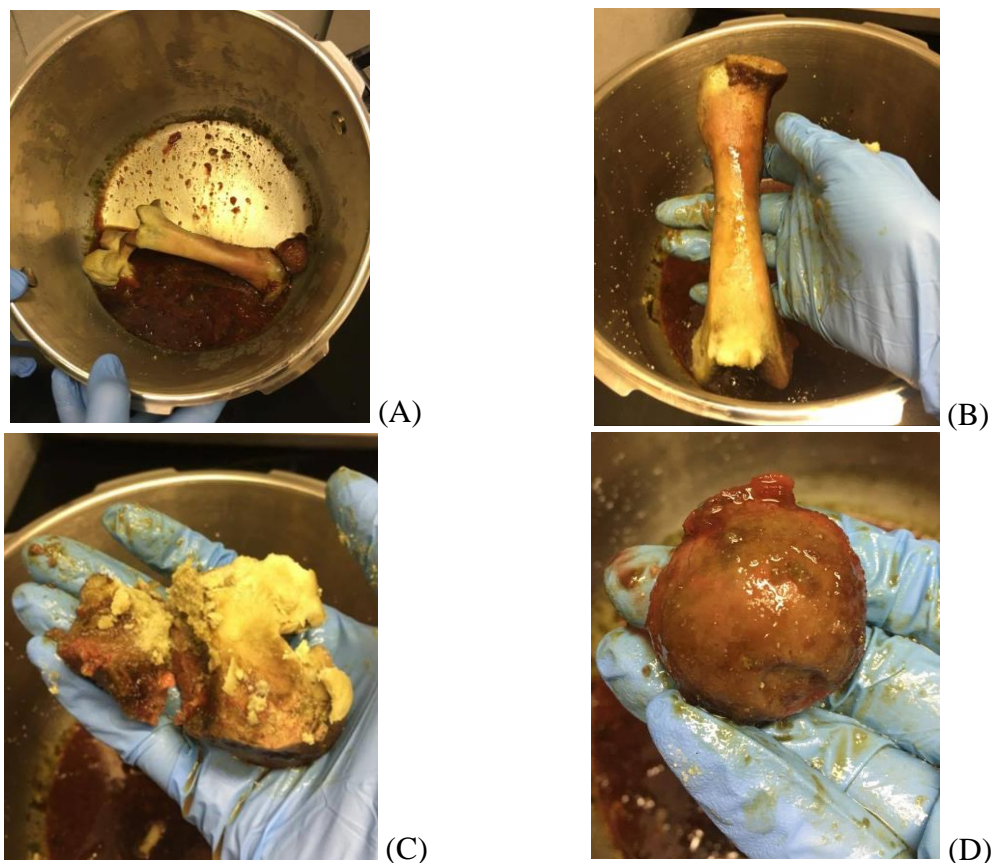


Figure 11: (A) remaining KOH solution and femur broken into three pieces. (B) main femur shaft with proximal and distal ends missing and slight red discoloration. (C) distal portion of femur, condyles, partially crushed. (D) proximal portion, femoral head.

Femur 2:

In response to the results of femur 1, an additional 1.5 liters of deionized water was added to fill the pressure cooker halfway to prevent the pot from running dry. A total of 30 mL of the KOH/H₂O sample were taken every thirty minutes for atomic absorption analysis and the water was replenished to the half-way mark with approximately 100 to 300 mL of deionized water in the pressure cooker after sample removal. Depressurization

began five minutes before each sample was taken. At the end of three hours, the solution was filtered to catch any bone particles and to retrieve the larger bone parts which can be seen below in Figure 12.

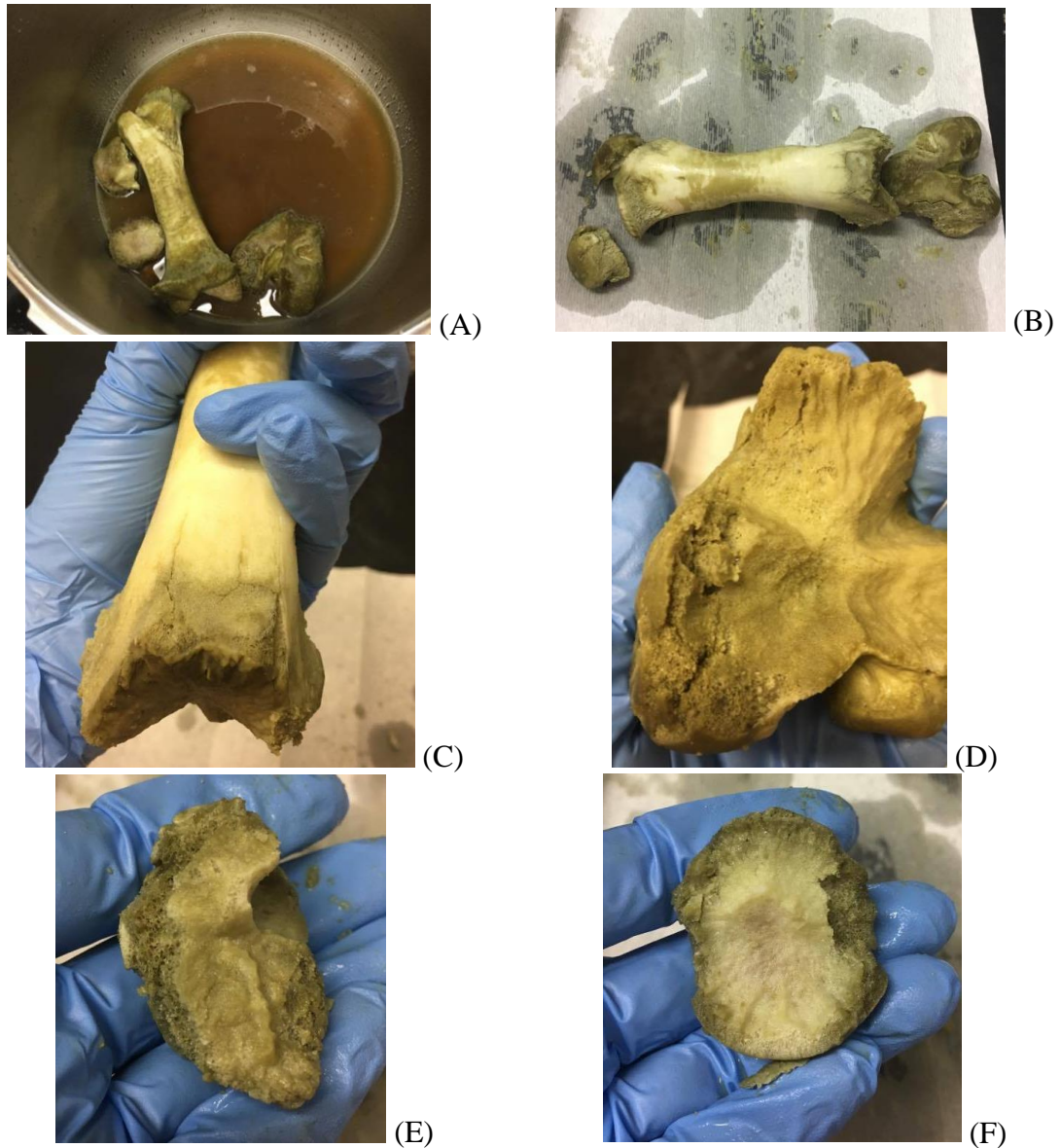


Figure 12: (A) femur broken into four parts. (B) relative placement of each epiphyseal surface to the femoral shaft and discoloration. (C) cracking and discoloration of distal femur. (D) cracking of epiphyseal surface of the medial condyle with discoloration. (E) greater trochanter with exposed spongy bone and discoloration. (F) femoral head showing discoloration halting at epiphyseal surface.

Atomic absorption (AA) spectroscopy was used to analyze a total of six sample solutions for calcium concentration of the pressure cooker solution. Figure 13 below shows the standard curve created for sample analysis. The curve ranged from 0.5 to 5 ppm with an extremely high linearity of 0.9979. Table 3 below shows the absorbance of each sample and their corresponding concentrations back-calculated to the original pressure cooker environment.

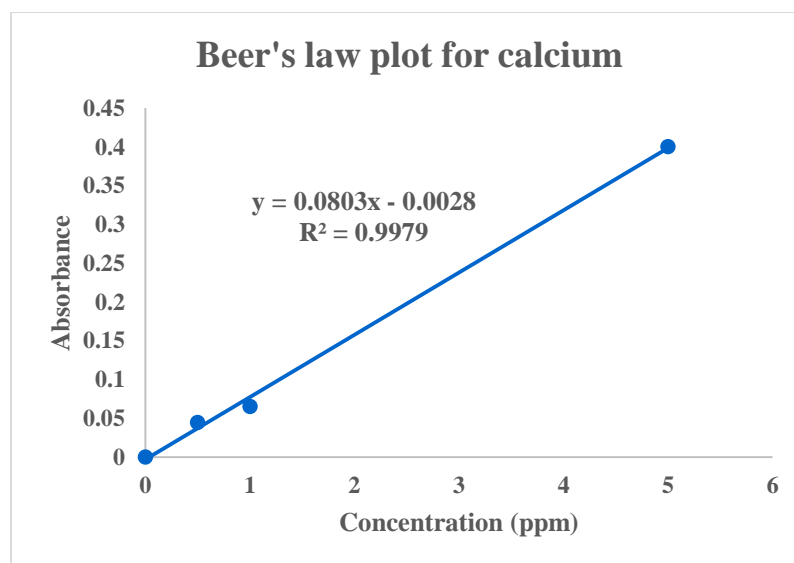


Figure 13: Beer's law standard curve created for calcium. The concentration of each solution was calculated using the linear regression equation in the graph above.

Femur 2 calcium concentration			
Collection Time (min)	Abs.	Concentration (ppm)	Concentration in original solution (ppm)
30	0.0486	0.640	560.1
60	0.0575	0.751	651.4
90	0.0597	0.778	669.4
120	0.0575	0.751	640.2
150	0.0516	0.677	730.8
180	0.0546	0.715	805.1

Table 3: Summation of sample absorbance and concentrations to original solution.

Femur 3:

No cremation was conducted on this femur due to the bone having decomposed too far since it was left too long in the refrigerator instead of freezer before it was used. The femur was eliminated to prevent the natural decomposition process from influencing the AHC process being performed.

Femur 4:

In an effort to fully cremate the bone, the cremation time was raised to four hours instead of three hours. The bone was partially frozen, inhibiting decomposition that occurred in femur 3, and was thawed fully before cremation. Two additional samples were extracted at 3 hrs and 30 minutes and 4 hrs and a third sample was added to the beginning at 0 minutes. Instead of removing 30 mL of sample, only 20 mL of sample were removed and 100 to 300 mL of deionized water was once again added to the halfway mark. The time zero sample was removed when the bone was placed in the KOH/H₂O solution and prior to heating and pressurization. Depressurization began five minutes before each sample was taken. During the third hour, banging noise was heard within the pressure cooker due to the bone bouncing around in the solution after additional water was added. The solution was filtered before the bones were removed. The bone results can be seen in Figure 14 below.

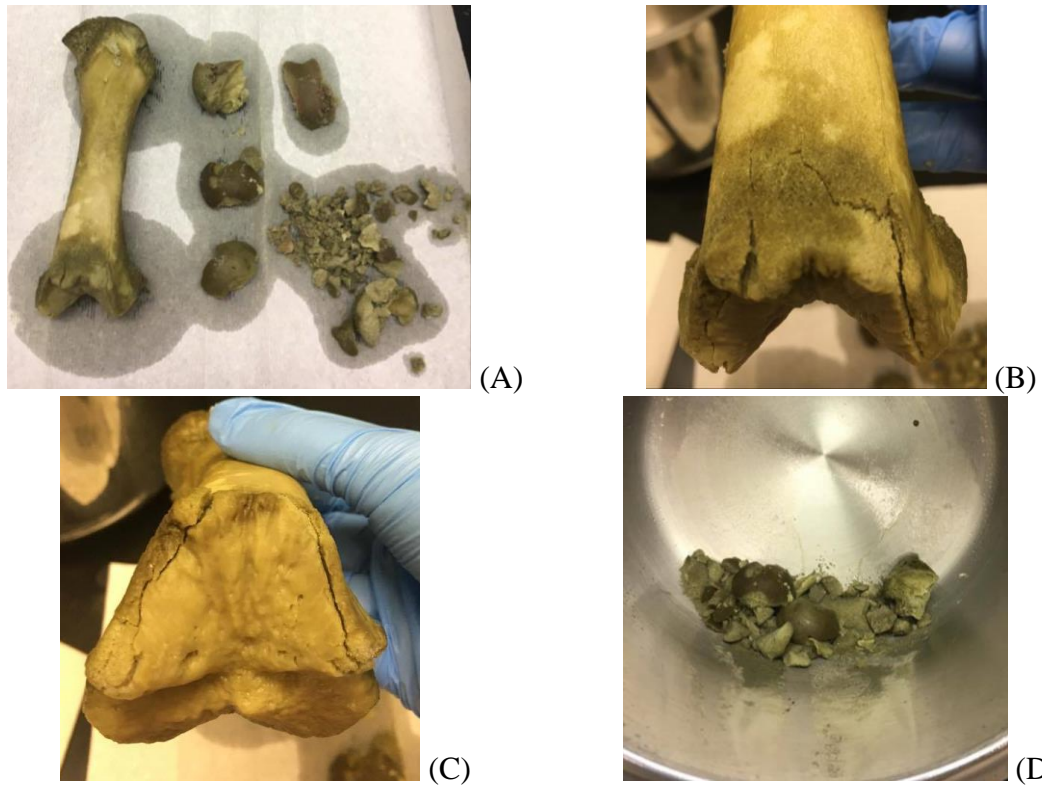


Figure 14: (A) remains of femur 4 after four hours of cremation with discoloration seen on the majority of the bones. (B) front view of distal femur showing extreme cracking and discoloration. (C) view of epiphyseal surface showing minimal discoloration and extensive cracking of sides. (D) remains of the femoral head, greater trochanter, and condyles.

Femur 4 was also left to dry completely to determine its brittleness and ease at which it could be crushed. The bone was left to air dry for five days and was examined for any changes to the color and structural integrity of the bone. Images of the bone can be seen in Figure 15 below.

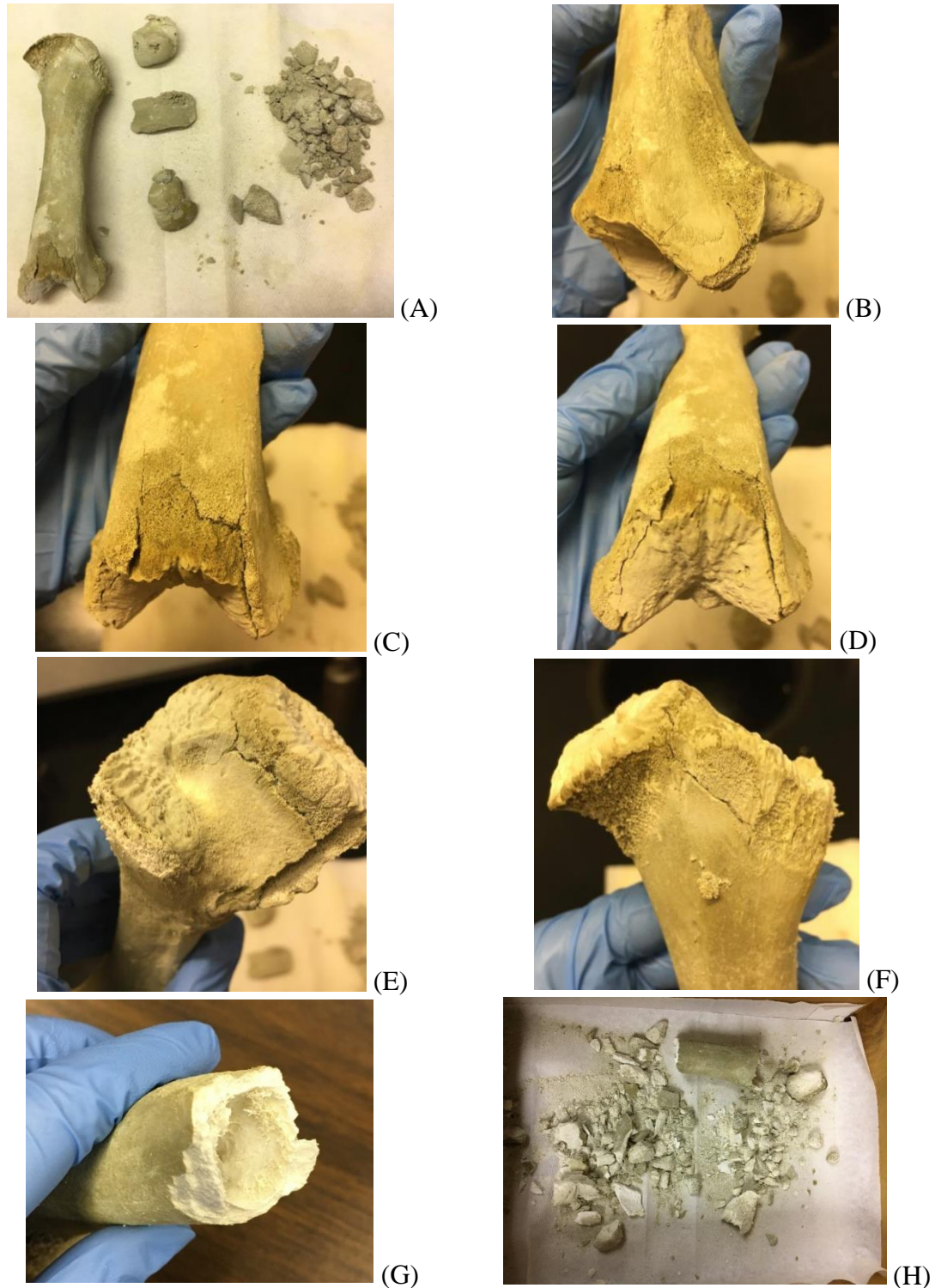


Figure 15: (A) remains of bones after drying for five days. (B) exposure of spongy and trabecular bone on the medial surface of the distal femur. (C) extended cracking of frontal femur. (D) bone peeling on the sides of the epiphyseal surface. (E) appearance of crack and gouge on the femoral neck. (F) crack extending downward on proximal femur. (G) empty marrow chamber. (H) remains of fully crushed femur 4.

Analysis of concentrations of calcium, iron, and magnesium was conducted by AA. The samples were acidified as stated in the experimental section in order to perform the analysis. Three standard curves were created to calculate the concentrations of the metals based on their specific absorbance. The curves and their corresponding equations can be seen in Figure 16 below. Iron was measured in the range of 0.1 to 0.5 ppm and magnesium ranged from 0.05 to 0.1 ppm with a high linearity of 0.9964 and 0.9933 respectively. Tables 4 through 6 display the absorbance and calculated concentration of each metal.

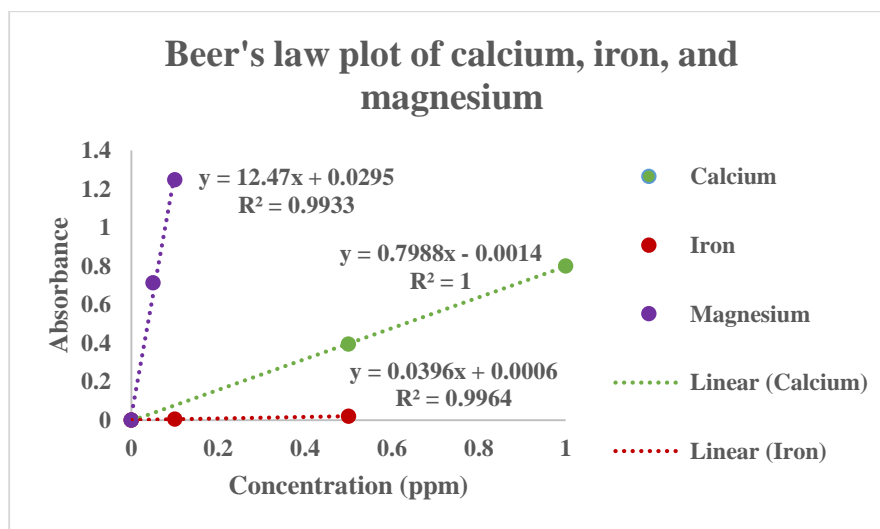


Figure 16: Combined standard curves for calcium, iron, and magnesium with corresponding linear regression equations used to calculate the concentration of each metal sample.

Femur 4 calcium concentration			
Collection Time (min)	Abs.	Concentration (ppm)	Concentration in original solution (ppm)
0	0.0568	0.0729	63.8
30	0.0264	0.0348	30.3
60	0.0369	0.0479	41.5
90	0.0336	0.0438	38.8
120	0.0359	0.0467	44.8
150	0.0330	0.0431	42.6
180	0.0507	0.0652	68.5
210	0.0313	0.0409	45.9
240	0.0837	0.1065	125.0

Table 4: Absorbance and corresponding calculated calcium concentrations in the sample and original pressure cooker solution.

Femur 4 iron concentration			
Collection Time (min)	Abs.	Concentration (ppm)	Concentration in original solution (ppm)
0	0.0020	0.0354	30.9
30	0.0014	0.0202	17.6
60	0.0014	0.0202	17.5
90	0.0018	0.0303	26.8
120	0.0023	0.0429	41.2
150	0.0028	0.0556	54.9
180	0.0028	0.0556	58.3
210	0.0030	0.0606	68.0
240	0.0019	0.0328	38.5

Table 5: Absorbance and corresponding calculated iron concentrations in the sample and original pressure cooker solution.

Femur 4 magnesium concentration			
Collection Time (min)	Abs.	Concentration (ppm)	Concentration in original solution (ppm)
0	0.179	0.0120	10.5
30	0.180	0.0121	10.5
60	0.379	0.0281	24.3
90	0.297	0.0214	19.0
120	0.238	0.0167	16.0
150	0.188	0.0127	12.6
180	0.104	0.00597	6.27
210	0.115	0.00682	7.65
240	0.182	0.0122	14.3

Table 6: Absorbance and corresponding calculated magnesium concentrations in the sample and original pressure cooker solution.

Discussion:

Femur 1:

As seen in Figure 11 (A), it appeared that all of the water had been cooked out of the solution. The resulting liquid would have consisted of KOH, collagen, and other organic substances which began to turn to a gelatinous substance that began to foam and exit through the release valve. The resulting bone revealed some interesting characteristics. The femur can be seen to have detached into three different parts, as seen in Figure 11 (A). The detachment points coincide with the epiphyseal or growth plate areas of the femur. Upon first inspection of the femur, it appeared to have fused epiphyses, meaning the condyles and head should not have detached as easily since they would have become one solid bone with the femoral shaft. This suggests that the pig was much younger than first thought, between two to three years at death.

In Figure 11 (B-D) the red discoloration is due to the bones sitting in the concentrated solution. The breakdown of the condyles in (C) is evidence of cremation.

The bone was fragile to pick up and the removal of the bone from the pot resulted in the damage. The edges of the proximal and distal femur in Figure 11 (B) as well as the head in (D) had a softer feel when compared to the femoral shaft which was still as firm as it was before the cremation. The softer feel to the bone is further evidence of cremation because those are the points where the hydroxyapatite crystal structure is weakest due to calcium removal. In these areas there is a large amount of trabecular bone at the epiphyses, increasing the surface area available for the KOH solution to react with. Therefore, the areas of the epiphyses will breakdown much faster than the rest of the bone.

Femur 2:

The cremation of femur 2 was performed for the full three hours since additional water was added to the pressure cooker and it did not run dry. The bone again separated into four different sections, the femoral head, greater trochanter, femoral shaft, and condyles. One difference between femur 1 and 2 is a green discoloration seen on the distal portion of the femur 2 shaft, as well as the condyles, greater trochanter, and outline of the femoral head. The placement of the green color coincides with the epiphyseal sites of the bone and is also where a large amount of blood vessels flow to provide blood to the growth plate. Therefore, the green discoloration is due to the breakdown of the haemin in the blood at the ends of the bone. Haemin breakdown is also known to transform into biliverdin and bilirubin which is green in color.²³

The bones also showed more extensive cracking and breakdown than femur 1. In Figure 12 (C) cracks are present on the anterior surface of the distal portion of the femur. Those cracks only extend as far as the green discoloration but were not present on

femur 1. In image (D), a large chunk of the condyle is crumbling and was able to be pulled off of the bone itself. In images (E) and (F), no cracking is present but the edges of the bone are ragged and spongy looking. This is due to the removal of the layer of dense bone, exposing the spongy bone below. These two bones show evidence of the KOH solution eating its way through the outer bone surface to begin impacting the softer, inner bone. This was not seen in femur 1. Since the reaction conditions were not equal for femur 1 and 2, there is no way to conclusively tell if the cracks and breakdown appeared due to the extra thirty minutes the bone was submerged in the KOH/H₂O solution. The combination of the green discoloration and the appearance of the breakdown of the bone can be used as indicators of the extent of cremation. The more discoloration of the bone as well as ragged, broken edges, the farther cremated the bone is.

The AA data, in Table 3, revealed a steady increase in calcium concentration throughout the 3 hours of cremation. This is consistent with the breakdown of the bone discussed previously. The absorbance and concentration seen in columns two and three correspond to the 25 mL diluted sample used in the AA analysis. The concentration in original solution in column four is the calcium concentration in the pressure cooker solution, including the water added after each sample was taken.

The slight decrease in calcium concentration between 90 and 120 minutes could be due to a decrease in the amount of calcium being removed from the bone while the sample collection removed the calcium from the solution. Another reason for this decrease can be the formation of a Ca(OH)₂ precipitate. The acidification process was used to dissociate the calcium and hydroxide, releasing the calcium back into solution for analysis. If the acidification did not release all of the calcium from the precipitate, a

lower absorbance, and therefore lower concentration of calcium, will be detected by the AA. This can be resolved by using a higher concentration of HNO_3 for acidification and will increase the amount of $\text{Ca}(\text{OH})_2$ that is dissociated.

Femur 4:

In an attempt to fully cremate femur 4, the cremation time was increased to 4 hours instead of 3. This resulted in the bone breakdown seen in Figure 14. The bone was broken into significantly more pieces during this cremation. The femur shaft remained intact but the condyles were completely destroyed, the remnants can be seen as the pile of bone in image (A and D). This was most likely due to the bone being thrown around in the solution and hitting other bone, as well as the sides of the pressure cooker, causing the already brittle bone to break apart much more easily. Similar evidence of bone breakdown was present on femur 4, as with femur 2, except it was more extensive in femur 4. In image (A) the discoloration covers all of the bones, with a small patch of the femur remaining a white color. Since the bone was in the $\text{KOH}/\text{H}_2\text{O}$ solution an additional hour, the blood within the bone was able to breakdown further in femur 4 than in femur 2.

In image (B) the discoloration is more concentrated in the lower half of the femur and the cracking appears almost identical to the cracks in femur 2, which extends to the edge of the discoloration. The cracking extends to the epiphyseal surface, which can be seen in image (C). The bone appears to be peeling away from the main shaft, extending laterally down the surface. All of the bones were extremely fragile and difficult to remove from the pressure cooker without causing additional damage. Unique to this bone was the condition of the femoral shaft. In femur 2, the shaft was very strong after three

hours and appeared to not have been greatly impacted by the KOH/H₂O solution. In femur 4, indents could be made in the shaft with a fingernail after removal from the solution. This is evidence of the solution breaching through the top layers of the trabecular bone and beginning to break down the hydroxyapatite structure.

Femur 4 was left to dry for five days to observe the bone structure both wet and dry. Those images can be seen in Figure 15. Image (A) shows all the bones fully dry. A color change occurred during this time with the entire bone taking on a grey/tan coloring as it dried. This could be due to any remaining KOH/H₂O solution drying on the outside of the bone while the inside remained pure white like in image (G). Images (B through D) show the distal end of the femur where the condyles were attached. The cracking that was previously present in the wet bone has become more prominent and bone appears to have broken off in some areas. Image (C) shows the appearance of spongy bone in the lower middle portion of the bone. This means the dense bone has broken down enough to leave the more porous bone underneath exposed or the basic solution ate away at the dense bone on top, leaving behind pockmarks on the surface to give the appearance of spongy bone.

In image (D) a chunk of the edge of the bone does appear to be missing, exposing the spongy bone, but does not extend back far enough to account for all of the pockmark-like bone. Therefore, the KOH solution did breakdown a section of the dense bone but had just begun to affect another section of the bone, leaving behind the pockmarks. A similar situation can be seen in image (B) on the medial surface of the distal femur, a strip of smooth, dense bone with sections of pockmarked bone on either side due to breakdown by KOH.

The proximal end of the femur seen in image (E and F) show cracking not previously present in the wet bone. The crack extends parallel to the femoral head on the posterior surface of the bone. A second crack can be seen running perpendicular to the femoral head on the anterior surface of the bone, extending to the greater trochanter. No other damage appeared in that area. Both ends of the bone were extremely fragile, and when squeezed, shattered with a little application of pressure, the results of which can be seen in image (H). The only part of the bone that remained intact was the central shaft seen in image (G). The central marrow channel was completely empty, meaning the marrow liquefied and leached out of the bone sometime during the cremation process and leaving behind the bone white coloring.

Full analysis of calcium, iron, and magnesium ion concentration was performed for femur 4, resulting in Tables 4 through 6 seen earlier. The fourth column shows the concentration of each metal in the original pressure cooker solution. A graph of concentration vs. time can be seen in Figure 17 below, comparing the three metal ion concentrations throughout the cremation process.

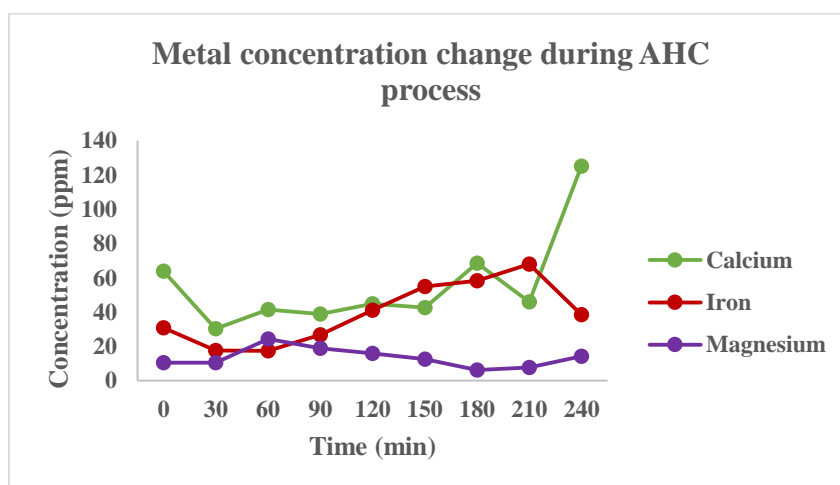


Figure 17: Graph comparing the concentrations of the three metals analyzed by atomic absorption spectroscopy.

The first trend that can be seen in the graph is the high initial concentration at 0 minutes. This can be due to the sample having been collected when the bone was placed in the KOH/H₂O solution and began to decompose the little amount of soft tissue that remained on the bone. After 30 minutes, the calcium and iron levels began to climb steadily until calcium decreased at 210 minutes and iron decreased at 240 minutes. This shows both calcium and iron were steadily removed from the bone structure over the course of the cremation, which could have been one component of the bone breakdown.

A comparison of the calcium concentrations between femur 2 and 4 shows that the calcium was removed throughout the whole cremation processes but the final concentrations were strikingly different. Femur 2 had a significantly higher calcium concentration over the entire cremation process and had a continuous increase over the full 3 hours. This can be due to the small difference in linear regression equations for each of the calcium samples. Even though the concentrations of calcium do not match for both femur bones, the trend still remains that calcium is removed throughout the cremation process.

An interesting aspect of the iron concentration (Table 5, Figure 17) is a dramatic increase in iron between 90 and 120 minutes. This is most likely the point where the bone marrow was liquefied and removed from the marrow channel within the bone. Since bone marrow is rich in blood, the breakdown of the hemoglobin would have released a large amount of iron into the solution, increasing its concentration. After 120 minutes, the iron levels began to rise slowly again.

The third metal investigated, magnesium, had a very different trend in concentration. Instead of an increasing concentration line, the line slowly decreases over

time after a peak at 60 minutes. This could be due to the magnesium not residing within the bone structure at all, but in the small amount of flesh present or even in the cartilage that decomposed rather quickly when exposed to the KOH/H₂O solution. This is the opposite of what was expected since the literature suggested magnesium played a key part in the stability of the bone crystal structure. Another reason for the low concentration could be the sensitivity of the instrument coupled with the sample being too diluted. The amount of magnesium in the diluted sample may have been within the sensitivity range of the instrument, causing it to register minimal changes in concentration over time.

Future work on this topic includes using scanning electron microscopy to obtain a visual representation of the inside of the bone structure before and after the cremation process. These images could provide additional evidence to determine what happens to the bone that causes it to breakdown. Additional cremations can also be performed for shorter time ranges to create a standardization of the bone breakdown at each stage of the cremation process as well as cremating fleshed specimens to see the variation in the process when flesh is added. Further investigating the trend seen in the magnesium sample can lend more insight into bone composition and structure. Research can also expand into other disciplines. Forensic anthropologists can analyze the bones to see what can be deciphered from them after cremation, environmental scientists can find ways to safely dispose of the alkaline solution, and mortuary scientists can further explore its use for full body cremations.

Conclusion:

Three pig femur bones were cremated using the alkaline hydrolysis cremation process to varying degrees of success. The second femur had portions of bones which

were able to be crushed without much force but did not achieve the complete cremation that was expected. The fourth femur reached full cremation where the bone, once dried, was crushed using only a strong squeeze of a hand. The analysis of the calcium, iron, and magnesium metals in the basic solution showed interesting results. The calcium and iron concentrations steadily increased throughout the entire AHC process but they decreased around the fourth hour of cremation. The results of magnesium were the opposite of what was expected. The magnesium concentration reached a maximum peak within 60 minutes of cremation and steadily decreased over the next three hours. This could be due to magnesium not being used internally within the bone structure as the literature suggested.

The successful cremation of two femur bones in four hours shows the ability to reduce the commercial process to a small scale apparatus that can be used in a lab setting. The results of the metal analysis show that the removal of calcium and iron are just one factor that contributes to bone breakdown.

References:

1. Pettitt, P. From funerary caching to the earliest burials of early *Homo sapiens*. In *The Paleolithic Origins of Human Burial*; Routledge: Milton Park, Abington, Oxon, 2011; 57-77.
2. "Statistics" 2016. National funeral Directors Association. <http://www.nfda.org/news/statistics>. (accessed Oct 30, 2016).
3. Kim, M. "How Cremation Works" 31 March 2009. HowStuffWorks.com. <http://science.howstuffworks.com/cremation.htm> (accessed Oct 18, 2016).
4. Schvaneveldt, J.D. *Utah State University Extension*. **1989**, Paper 451, 1-3.
5. Rumble, H., Troyer, J., Walter, T., Woodthorpe, K. *Mortality*. **2014**, 19(3), 243-260.
6. Olson, P.R. *Science, Technology, & Human Values*. **2014**, 39(5), 666-693.
7. Rylands, T. "Alkaline Hydrolysis: Water Cremation and the 'Ick Factor'" 22 July 2014. Confessions of a Funeral Director. <http://www.calebwilde.com/2014/07/alkaline-hydrolysis-water-cremation-and-the-ick-factor/> (accessed Oct 18, 2016).

8. Sickel, J. "Liquid cremation gains foothold amid obstacles" 9 August 2012. Online Athens. <http://onlineathens.com/faith/2012-08-09/liquid-cremation-gains-foothold-amid-obstacles#> (accessed Oct 18, 2016).
9. Baumen, P.A., Lawrence, L.A., Biesert, L., Dichtelmüller, H., Fabbrizzi, F., Gröner, A., Jorquera, J.I., Kempf, C., Kreil, T.R., von Hoegen, I., Pifat, D.Y., Petteway Jr, S.R., Cai, K. *Vox Sanguinis*. **2006**, *91*, 34-40.
10. Clarke, B. *Clin J Am Soc Nephrol*. **2008**, *3*(3), S131-S139.
11. "An Inside Look at Bone" Smithsonian National Museum of Natural History. https://anthropology.si.edu/writteninbone/inside_look.html 18 October 2016.
12. The Editors of Encyclopedia Britannica. Osteon. *Encyclopedia Britannica* [Online]; Encyclopedia Britannica, inc. <https://www.britannica.com/science/osteon>. (accessed Oct 18, 2016).
13. The Arizona Science Center, "Busy Bones" 4 February 2011. ASU – Ask A Biologist. <https://askbiologist.asu.edu/bone-anatomy> (accessed Oct 18, 2016).
14. White, T.D., Black, M.T., Folkens, P.A. Bone Biology and Variation. In *Human Osteology*; Brown, L., Anderson, K., Eds.; Academic Press: Burlington, 2011; Third Edition, 25-42.
15. Maciejewska, K., Drazaga, Z., Kaszuba, M. *International Union of Biochemistry and Molecular Biology*. **2014**, *40*(4), 425-435.
16. Boivin, G. *Medicographia*. **2007**, *29*(2), 126-132.
17. Vallet-Regí, M., González-Calbet, J.M. *Progress in Solid State Chemistry*. **2004**, *32*, 1-31.
18. Ren, F., Lu, X., Leng, Y. *Journal of the Mechanical Behavior of Biomedical Materials*. **2013**, *26*, 59-67.
19. Castiglioni, S., Cazzaniga, A., Albisetti, W., Maier, J.A.M. *Nutrients*. **2013**, *5*, 3022-3033.
20. Mao, Z., Yang, X., Zhu, S., Cui, Z., Li, Z. *Ceramics International*. **2015**, *41*(3), 3461-3468.
21. Harris, D.C. Chapter 20: Atomic Spectroscopy. *Quantitative Chemical Analysis* 8th edition, 479-492.
22. Wang, T., Wu, J., Yi, Y., Qi, J. *Procedia Environmental Sciences*. **2016**, *31*, 366-374.
23. Lemberg, R., Wyndham, R.A. *Biochem J*. **1936**, *30*(7), 1147-1170.

Appendix A: Trauma Analysis Pictures

Femur 1:



(A)



(B)

Figure 18: (A) Slice to the posterior medial condyle, impacting the trabecular bone only. (B) Superficial slice to the medial surface of head, extending slightly to the neck.

Femur 2:



(A)



(B)

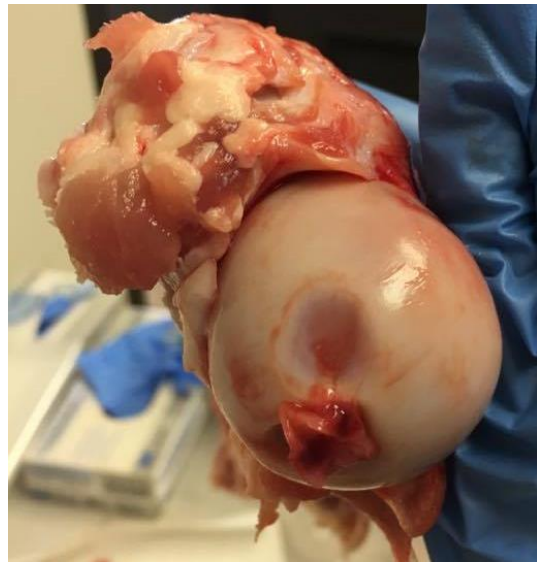
Figure 19: (A) Superficial slice to the medial surface of the femoral head, impacting the cartilage. (B) Slice to the posterior lateral condyle, impacting the trabecular bone only.

Femur 3:

Figure 20: Slight shave off of the medial condyle, more so than the lateral condyle, impacting the trabecular bone.

Femur 4:

(A)



(B)

Figure 21: (A) Slight laceration on the head, extending to the neck. (B) Scrape off the top head exposing trabecular bone.